



Title	STRUCTURE OF COMMERCIAL IRON CATALYST UNDER AMMONIA DECOMPOSITION : Part 2. Studies on X-ray Reflection Intensity and Line-breadths of $\alpha$ - and $\beta$ -Phases
Author(s)	MATSUI, Toshiji; TOYOSHIMA, Isamu
Citation	JOURNAL OF THE RESEARCH INSTITUTE FOR CATALYSIS HOKKAIDO UNIVERSITY, 10(3), 189-202
Issue Date	1962-12
Doc URL	<a href="http://hdl.handle.net/2115/24763">http://hdl.handle.net/2115/24763</a>
Type	bulletin (article)
File Information	10(3)_P189-202.pdf



[Instructions for use](#)

# STRUCTURE OF COMMERCIAL IRON CATALYST UNDER AMMONIA DECOMPOSITION

## Part 2. Studies on X-ray Reflection Intensity and Line-breadths of $\alpha$ - and $\gamma'$ -Phases

By

Toshiji MATSUI and Isamu TOYOSHIMA<sup>\*)</sup>

(Received Aug. 1, 1962)

### Abstract

The catalysts have been examined by x-ray diffraction at three typical points on the hysteresis loop of the rate of steady decomposition of ammonia, revealed by decreasing and then increasing constant hydrogen inflow rate  $N_H$  stepwise at fixed inflow rate of ammonia  $N_A$  over doubly promoted iron catalyst kept at constant temperature around 450°C. The catalysts examined are the same as those in the previous work, i.e. that (Catalyst-I) at point  $N_H/N_A=0$ , that (Catalyst-II) at point  $N_H/N_A=1$  on the lower curve of the loop observed on increasing  $N_H$  and that (Catalyst-III) at point  $N_H/N_A=1$  on the upper curve of the loop observed on decreasing  $N_H$ .

The observed increase of integrated intensity along the line of flow in  $\gamma'$ -phase of Catalyst-I was found to be attributable to decrease of excess nitrogen atoms over the stoichiometric composition of  $\text{Fe}_4\text{N}$ . The gradual decrease of intensity towards the outlet of the catalyst bed observed with  $\alpha$ -phase of Catalyst-III was not similarly explicable on the basis of "frozen heat motion" as in the case of  $\gamma'$ -phase of Catalyst-I. The observed line-breadth was analysed by CAUCHY's relation and shown to be attributable to small size of crystallite as well as to lattice strain. The causes of the strain were discussed briefly.

### § 1 Introduction

The steady decomposition of ammonia was observed by TOYOSHIMA and HORIUTI<sup>1)</sup> by allowing mixture of ammonia and hydrogen over an ammonia synthetic catalyst bed at constant temperature around 450°C and constant flow rate of the respective gases. The fraction of ammonia decomposed was thus followed until the fraction became steady at each constant inflow rate  $N_H$  of hydrogen, which was then stepwise decreased from *ca.* 4  $N_A$  to zero and then similarly increased, with the inflow rate  $N_A$  of ammonia kept constant throughout. It was thus found that the steady fraction of ammonia decomposition

<sup>\*)</sup> T. M. and I. T.: Research Institute for Catalysis, Hokkaido University.

plotted against  $N_H/N_A$  revealed a stable and reproducible hysteresis loop between  $N_H/N_A = 0.5$  and  $N_H/N_A = 4$ , the steady fraction being higher on decreasing  $N_H/N_A$ .

MATSUI and TOYOSHIMA<sup>2)</sup> have examined the catalysts by x-ray diffraction at the three typical points on the hysteresis loop, *i.e.* those at  $N_H/N_A = 0$  (Catalyst-I), at  $N_H/N_A = 1$  (Catalyst-II) on the lower curve of the loop and at  $N_H/N_A = 1$  (Catalyst-III) on the upper curve of the loop. The constituent phases identified of the catalyst at each point on the hysteresis loop were found, as reported in the previous paper<sup>2)</sup>, to be in good agreement with those concluded by TOYOSHIMA and HORIUTI from the kinetic analysis of the hysteresis loop on the basis of the ammonia decomposition mechanism advanced by HORIUTI *et al.*<sup>3)</sup>. It was found<sup>2)</sup> that Catalyst-I consisted solely of  $\gamma'$ -phase ( $\text{Fe}_4\text{N}$ ) except just at the inlet of the bed, where a small amount of  $\epsilon$ -phase ( $\text{Fe}_3\text{N}$ ) coexisted with main  $\gamma'$ -phase. Catalyst-II, on the other hand, was composed solely of  $\gamma'$ -phase or  $\alpha$ -phase at the inlet or the outlet of the bed, both the phases coexisting at the middle. Catalyst-III was similarly composed solely of  $\alpha$ -phase except at the inlet of the bed, where a minute amount of  $\gamma'$ -phase was found to coexist with main  $\alpha$ -phase.

It was further found that the lattice parameter of  $\gamma'$ -phase in Catalyst-I decreased slightly along the line of flow. In cases of Catalyst-II and Catalyst-III, significant change in the lattice parameter along the flow was not ascertained as in the case of Catalyst-I on account of larger experimental error due to the overlap of  $\alpha$ -doublet attributable to finer crystallite size. It was now consistently concluded<sup>2)</sup> from the above observations on the composition and the lattice parameter of catalyst at least in the case of Catalyst-I that the nitrogen content in catalyst decreases along the line of flow.

The present work is devoted to the following investigation of the above conclusion on nitrogen content in the catalyst by intensity measurement of x-ray diffraction pattern: the unit cell of  $\gamma'$ -phase, according to JACK<sup>4)</sup>, is cubic with four iron atoms at  $000$ ,  $\frac{1}{2}\frac{1}{2}0$ ,  $\frac{1}{2}0\frac{1}{2}$  and  $0\frac{1}{2}\frac{1}{2}$  and one nitrogen atom at  $\frac{1}{2}\frac{1}{2}\frac{1}{2}$ . There are three other possible equivalent sites for nitrogen atom within the unit cell at  $\frac{1}{2}00$ ,  $0\frac{1}{2}0$  and  $00\frac{1}{2}$ , which are left unoccupied. Excess nitrogen atoms over the stoichiometric composition of  $\text{Fe}_4\text{N}$  will therefore locate randomly over the latter group of sites, hence give rise to random displacement of the surrounding iron atoms resulting in decrease of intensity of reflection similar to that caused by heat motion in lattice. To describe such an effect of random displacement of atoms on reflection intensity, HENGSTENBERG and MARK<sup>5)</sup> introduced the concept of "frozen heat motion". In case of the  $\alpha$ -phase the nitrogen atoms randomly occupying octahedral interstices will give rise to

the similar effect, hence to decrease of reflection intensity. Non-uniform distribution of nitrogen atoms in catalyst will on the other hand result in lattice strain hence in broadening of reflection line, which is another subject of the present experimental investigation.

## § 2 Experimental

The specimens used in the present work are the same as those used in the previous one: Catalyst-I was the catalyst bed at the point  $N_H/N_A = 0$ , Catalyst-II that at the point  $N_H/N_A = 1$  on the lower curve of the loop and Catalyst-III that at the point  $N_H/N_A = 1$  on the upper curve. Each catalyst bed was divided in consecutive layers across the line of flow and each layer was examined as follows, after being powdered in agate mortar or as it was, if sufficiently powdered as in the case of Catalyst-I by repeated hysteresis observations. The powdered catalyst was pressed into specimen holder of diffractometer at approximately constant pressure. The holder was rotated about the axis perpendicular to the diffractometer axis and normal to the face of the holder during the measurement of line profile. The line profile was recorded by means of strip-chart recording method, using filtered Co-K $\alpha$  radiation. The voltage input to the x-ray tube was maintained at 35 kV and the tube current at 7 mA throughout all the measurements by means of electronic stabilizer as in the previous work<sup>2)</sup>. The conter circuit was subjected to frequent checks of stability by examining the constancy of x-ray count at fixed position of the counter.

*Integrated intensity.* Integrated intensity of reflection was determined by measuring the area of the line profile corrected for counting-loss due to dead-time of the Geiger-counter circuit above background-level. The background-level was taken to be the constant intensity determined at angles sufficiently remote from that of the reflection<sup>\*)</sup>.

*Line-breadth.* Intrinsic line-breadth ( $\beta$ ) of reflection line was determined according to JONES<sup>6)</sup> from observed integral breadth ( $\beta_0$ ) defined as  $\beta_0 = \text{Integrated intensity of reflection/Peak height}$ , using well-annealed powder of silicon metal for correction of the instrumental breadth. If the line broadening is due only to small size of crystallites, the intrinsic breadth  $\beta$  thus determined would assume the value  $\beta_p$ , *i. e.*

$$\beta_p = \lambda/\varepsilon_0 \cos \theta^{6)},$$

---

\*) In case where the background-levels both at the remote angles are not coincident, they were connected with a sloped straight line drawn against the angle to give the background-level at each angle.

whereas if the broadening were caused solely by lattice strain,  $\beta$  would equal  $\beta_s$ , *i.e.*

$$\beta_s = 2 \eta \tan \theta^\gamma,$$

where  $\varepsilon_0$  is the mean thickness of crystallite in the direction of normal to the reflecting plane and  $\eta$  the integral breadth of distribution function of strain. The line-breadth  $\beta$  due both to these causes is now expressed by CAUCHY's relation as found by HALL<sup>8)</sup> and HALL and WILLIAMSON<sup>9)</sup> as

$$\beta \cos \theta / \lambda = 1 / \varepsilon_0 + 2 \eta \sin \theta / \lambda. \quad (1)$$

The above equation shows that  $1/\varepsilon_0$  and  $\eta$  are determined as the intercept and the slope of the plot of  $\beta \cos \theta / \lambda$  against  $2 \sin \theta / \lambda$ .

### § 3 Results and Discussions

#### 1. Integrated intensity

Fig. 1 shows the ratio  $I_n(\text{hkl})/I_1(\text{hkl})$  plotted against the number  $n$  of a layer of the catalyst bed along the line of flow, where  $I_1(\text{hkl})$  or  $I_n(\text{hkl})$  is the integrated intensity of (hkl)-reflection from the 1-st or  $n$ -th layer respectively. The results obtained with Catalyst-I, -II and -III are individually commented upon below.

*Catalyst-I.* Fig. 1 (a) shows the ratios for all the observed reflections, *i.e.*  $I_n(111)/I_1(111)$ ,  $I_n(200)/I_1(200)$ ,  $I_n(220)/I_1(220)$ ,  $I_n(311)/I_1(311)$  and  $I_n(222)/I_1(222)$ , plotted against the number  $n$  of layer. The catalyst consisted, as observed in the previous work, almost exclusively of  $\gamma'$ -phase with a small amount of  $\varepsilon$ -phase coexisting just at the inlet of the bed. The rate of increase of  $I_n(\text{hkl})/I_1(\text{hkl})$  with  $n$  is small at around  $n=5$  as compared with that at other  $n$ -values, as seen in the figure. The first rapid increase is attributable to the increase of fraction of  $\gamma'$ -phase in the catalyst,  $\varepsilon$ -phase observable at the inlet disappearing in subsequent layers. The second rapid increase is not similarly explicable because of the absence of  $\varepsilon$ -phase but alternatively on the basis of "frozen heat motion" as follows.

Nitrogen content of the  $\gamma'$ -phase at the inlet should be in excess of the stoichiometric composition of  $\text{Fe}_4\text{N}$  because of the coexistence of  $\varepsilon$ -phase, but decrease along the flow in accordance with the result of the lattice parameter measurement in the previous work<sup>2)</sup>. Let now  $\langle u_1^2 \rangle$  and  $\langle u_2^2 \rangle$  be the components of the mean square displacements of iron atoms in the direction normal to reflecting plane due to heat motion and the excess nitrogen respectively. Assuming that both the displacements are independent of each other, the total displacement  $\langle u^2 \rangle$  is written as

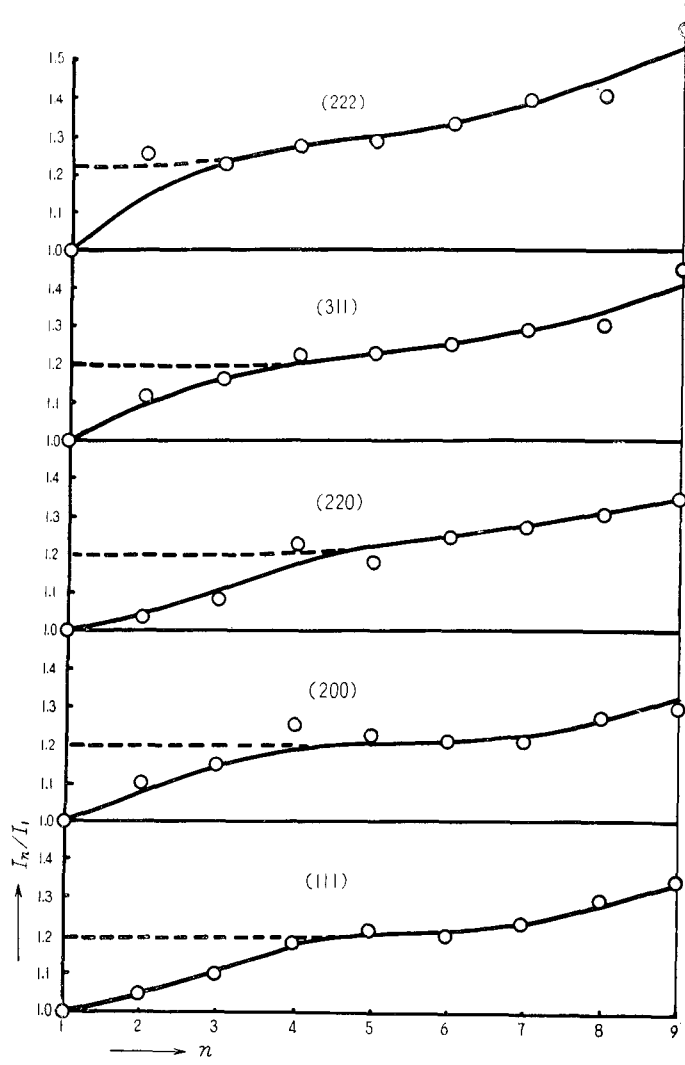


Fig. 1 (a).  $I_n/I_1$  plotted against the number  $n$  of layer.  $r'$ -phase of Catalyst-I. Dotted lines show extrapolation of second stage of increase at  $n=1$ .

$$\langle u^2 \rangle = \langle u_1^2 \rangle + \langle u_2^2 \rangle ,$$

hence DEBYE-WALLER factor in this case is given as

$$\begin{aligned} & \exp \left[ -8 \pi^2 \langle u^2 \rangle (\sin \theta / \lambda)^2 \right] \\ &= \exp \left[ -8 \pi^2 \langle u_1^2 \rangle (\sin \theta / \lambda)^2 \right] \cdot \exp \left[ -8 \pi^2 \langle u_2^2 \rangle (\sin \theta / \lambda)^2 \right] . \end{aligned}$$

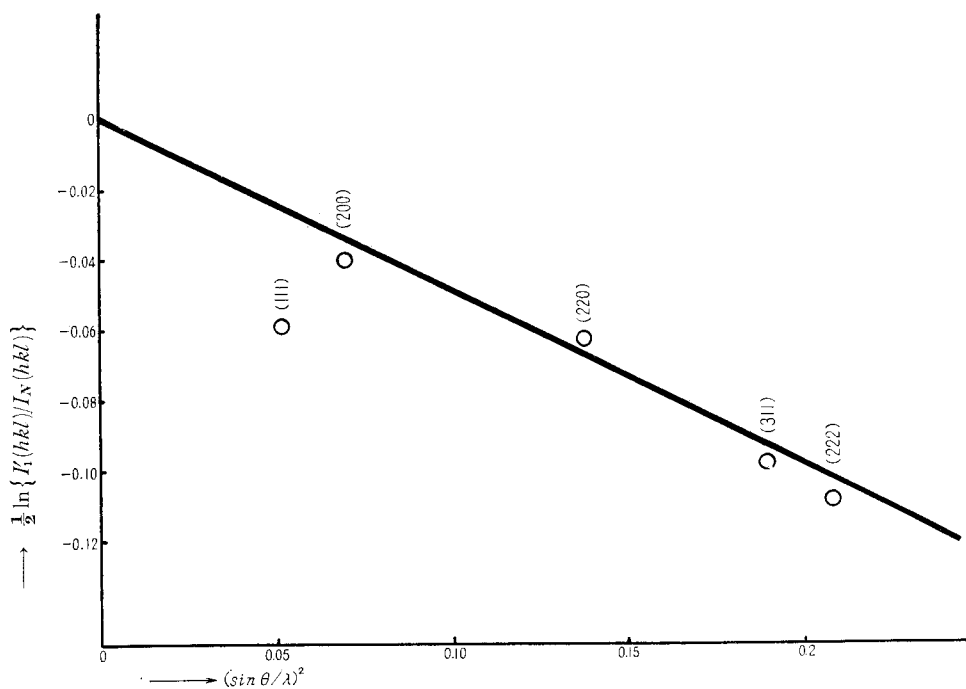


Fig. 2.  $\frac{1}{2} \ln \frac{I'(hkl)}{I_N(hkl)}$  vs.  $\left(\frac{\sin \theta}{\lambda}\right)^2$ .  $r'$ -phase of Catalyst-I.

Atomic scattering factor  $f_{Fe}$  of iron is now

$$f_{Fe} = f_{FeT} \exp \left[ -8 \pi^2 \langle u_2^2 \rangle (\sin \theta / \lambda)^2 \right],$$

where

$$f_{FeT} = f_0 \exp \left[ -8 \pi^2 \langle u_1^2 \rangle (\sin \theta / \lambda)^2 \right]$$

is atomic scattering factor with the heat motion alone taken into account. Ignoring contribution of nitrogen atoms to the intensity of reflection, structure factor  $F(hkl)$  is given as

$$F(hkl) = 4 f_{FeT} \exp \left[ -8 \pi^2 \langle u_2^2 \rangle (\sin \theta / \lambda)^2 \right], \quad (2. a)$$

where h, k, and l are all either even or odd numbers. The structure factor  $F_0(hkl)$  in the absence of excess nitrogen is obtained from Eq. (2. a) by equating  $\langle u_2^2 \rangle$  to zero as

$$F_0(hkl) = 4 f_{FeT}. \quad (2. b)$$

The ratio of intensity  $I(hkl)$  of (hkl)-reflection from  $r'$ -phase with excess nitrogen to that  $I_0(hkl)$  without the excess is now given by Eqs. (2. a) and (2. b) as

$$\begin{aligned} \left\{ I(\text{hkl})/I_0(\text{hkl}) \right\}^{\frac{1}{2}} &= F(\text{hkl})/F_0(\text{hkl}) \\ &= \exp \left[ -8\pi^2 \langle u_z^2 \rangle (\sin \theta / \lambda)^2 \right]. \end{aligned} \quad (3)$$

Fig. 2 shows the plot of  $\frac{1}{2} \ln \{I'_1(\text{hkl})/I_N(\text{hkl})\}$  against  $(\sin \theta / \lambda)^2$ , where  $I_N(\text{hkl})$  is the value of  $I(\text{hkl})$  of the layer at the outlet identified with  $I_0(\text{hkl})$ , and  $I'_1(\text{hkl})$  is the intensity at the second stage of increase extrapolated at  $n=1$  as shown by dotted lines in Fig. 1 (a). We see from Fig. 2 that the values of  $\frac{1}{2} \ln \{I'_1(\text{hkl})/I_N(\text{hkl})\}$  except that of (111) are scattered near a straight line through the origin, which means that the mean square displacement  $\langle u_z^2 \rangle$  is independent on the direction of normal to the reflecting plane, hence the displacement of iron atom caused by the excess nitrogen atom is isotropic. Therefore,  $\langle u_z^2 \rangle$  in Eq. 3 should be replaced by  $\langle U^2 \rangle / 3$ , where  $\langle U^2 \rangle$  is the mean square displacement of the iron atoms. The second rapid increase was thus accounted for on the basis of "frozen heat motion", confirming the decrease of nitrogen content of the  $\gamma'$ -phase along the line of flow. The root mean square displacement  $\sqrt{\langle U^2 \rangle}$  is estimated by Eq. (3) from the slope at 0.13 Å to 0.14 Å.

**Catalyst-II.** It has been observed in the previous work<sup>2)</sup> that the catalyst was composed solely of  $\gamma'$ -phase in layers near the inlet of catalyst bed, but replaced in subsequent layers gradually by  $\alpha$ -phase towards the outlet and completely there. The ratio  $I_n(\text{hkl})/I_1(\text{hkl})$  of the  $\gamma'$ -phase decreases with  $n$  in accordance with the above observation as seen in Fig. 1 (b), while the ratio  $I_n(\text{hkl})/I_N(\text{hkl})$  of  $\alpha$ -phase increases with  $n$ , where  $I_N(\text{hkl})$  is integrated intensity at the outlet of the bed.

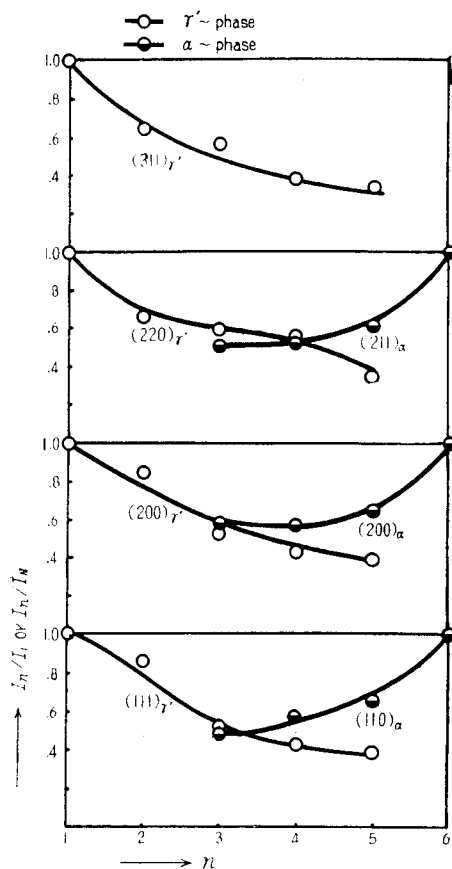


Fig. 1 (b).  $I_n/I_1$  plotted against the number  $n$  of layer.  $\gamma'$ - and  $\alpha$ -phases of Catalyst-II.



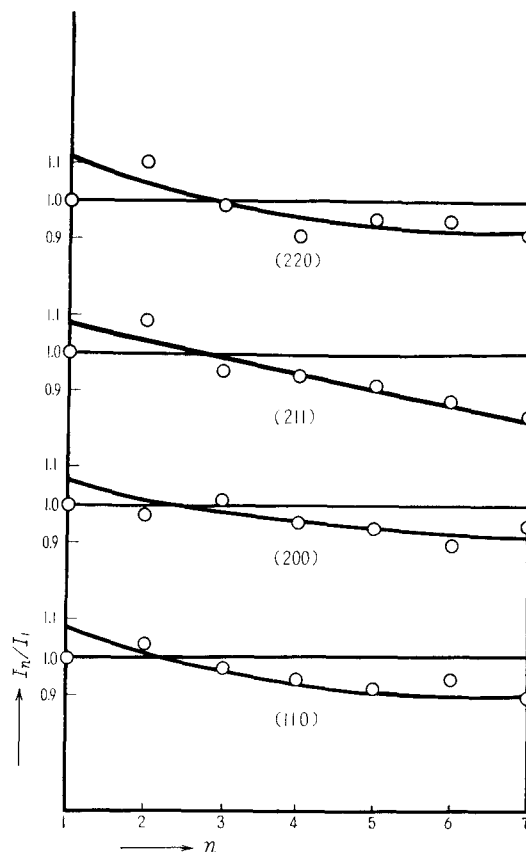


Fig. 1 (c).  $I_n/I_1$  plotted against the number  $n$  of layer.  $\alpha$ -phase of Catalyst-III.

*Catalyst-III.* The ratio  $I_n(hkl)/I_1(hkl)$  of  $\alpha$ -phase in this sample reveals a tendency to decrease monotonously towards the outlet of catalyst bed, as seen in Fig. 1 (c). This decrease is not explicable as in the case of  $\gamma'$ -phase in Catalyst-II, the catalyst being composed solely of  $\alpha$ -phase except just at the inlet of the bed, where  $\gamma'$ -phase coexists faintly with the main  $\alpha$ -phase. Neither was it attributable to the "frozen heat motion" as in the case of  $\gamma'$ -phase in Catalyst-I.

## 2. Line-breadth

The value of  $\beta \cos \theta/\lambda$  was practically constant along the line of flow for the reflection each of (111) *etc.* of the  $\gamma'$ -phase of Catalyst-I; Fig. 3 shows the plot of  $\beta \cos \theta/\lambda$  against  $2 \sin \theta/\lambda$ . The crystallite size and the lattice strain in (111)-direction are determined according to Eq. (1) from the intercept and the slope of a straight line through the points of (111) and (222), to which other points lie close as seen in the figure. It follows from the result that the

crystallites are approximately spherical and the strain isotropic. The  $\gamma'$ -phase in Catalyst-II gives similar straight lines as seen in Fig. 4 (a) except that the values of  $\beta \cos \theta/\lambda$  of Catalyst-II-5 are markedly scattered, which is attributable to the poor accuracy of intensity measurement due to the small fraction of  $\gamma'$ -phase in this layer.

No such linear relation was observed between  $\beta \cos \theta/\lambda$  and  $2 \sin \theta/\lambda$  in the case of  $\alpha$ -phase of Catalyst-II and Catalyst-III. The strain is unlikely to be isotropic because of the elastic anisotropy of  $\alpha$ -iron. The experimental result was now examined alternatively assuming isotropic stress in the crystallite. The value of  $\beta \cos \theta/\lambda$  was thus plotted against  $2 \sin \theta/E_{hkl}\lambda$  in place of  $2 \sin \theta/\lambda$ , where  $E_{hkl}$  is YOUNG's modulus of  $\alpha$ -iron in (hkl)-direction. The slope of the plot determines now integral breadth  $\sigma$  of the stress distribution function. Figs. 4 (b) and 5 show these plots with straight lines drawn through (110) and (220). The plots thus obtained are in accordance with the Cauchy's relation Eq. (1). The values of  $\epsilon_0$  and  $\eta$  or  $\sigma$  determined are listed in Table 1. Assuming CAUCHY's distribution of strain, mean of absolute strain  $\langle |s| \rangle$  is given

TABLE 1. List of values of  $\epsilon_0$ ,  $\sigma$ ,  $\eta$ ,  $\langle |s| \rangle$  and  $\langle |\Delta a_0| \rangle$

Catalyst	No. of layer	phase	$\epsilon_0$ (Å)	$\sigma \times 10^{-8}$ (dynes/cm <sup>2</sup> )	$\eta \times 10^3$	$\langle  s  \rangle \times 10^4$	$\langle  \Delta a_0  \rangle \times 10^3$ (Å)
I-	1, 2...9	$\gamma'$	3300	—	1.1	5.5	2.1
II-	1, 2, 3	$\gamma'$	312	—	1.4	7.0	2.7
"	4	$\gamma'$	377	—	1.1	5.5	2.1
"	5	$\gamma'$	—	—	—	—	—
"	3	$\alpha$	408	56	4.3	22	6.2
"	4	$\alpha$	455	58	4.4	22	6.2
"	5	$\alpha$	420	38	2.9	15	4.2
"	6	$\alpha$	400	34	2.6	13	3.7
III-	1	$\alpha$	—	—	—	—	—
"	2	$\alpha$	400	80	6.1	31	8.7
"	3	$\alpha$	—	—	—	—	—
"	4	$\alpha$	435	90	6.8	34	9.8
"	5	$\alpha$	—	—	—	—	—
"	6	$\alpha$	—	—	—	—	—
"	7	$\alpha$	455	84	6.4	32	9.1
"	7 (coarse)	$\alpha$	455	50	3.9	20	5.7

$\eta$  of  $\alpha$ -phase was calculated from  $\sigma$  with reference to YOUNG's modulus of  $\alpha$ -iron in (100)-direction;  $1.316 \times 10^{12}$  dynes/cm<sup>2</sup>.

approximately as  $\langle |s| \rangle \approx \frac{1}{2}\eta$ . The values of  $\langle |s| \rangle$  are summarized in the fifth column of the Table and the corresponding values of  $\langle |\Delta a_0| \rangle$  in the last column, where  $s = \Delta a_0/a_0$ .

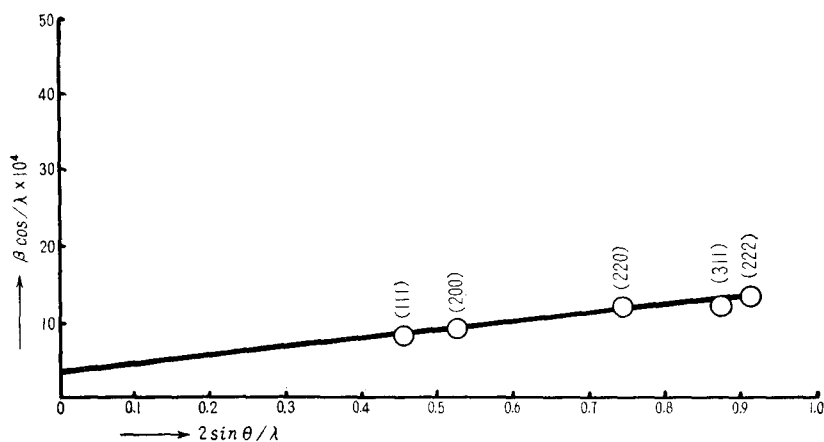


Fig. 3. Variation of  $\beta \cos \theta / \lambda$  with  $2 \sin \theta / \lambda$  for  $r'$ -phase of Catalyst-I.

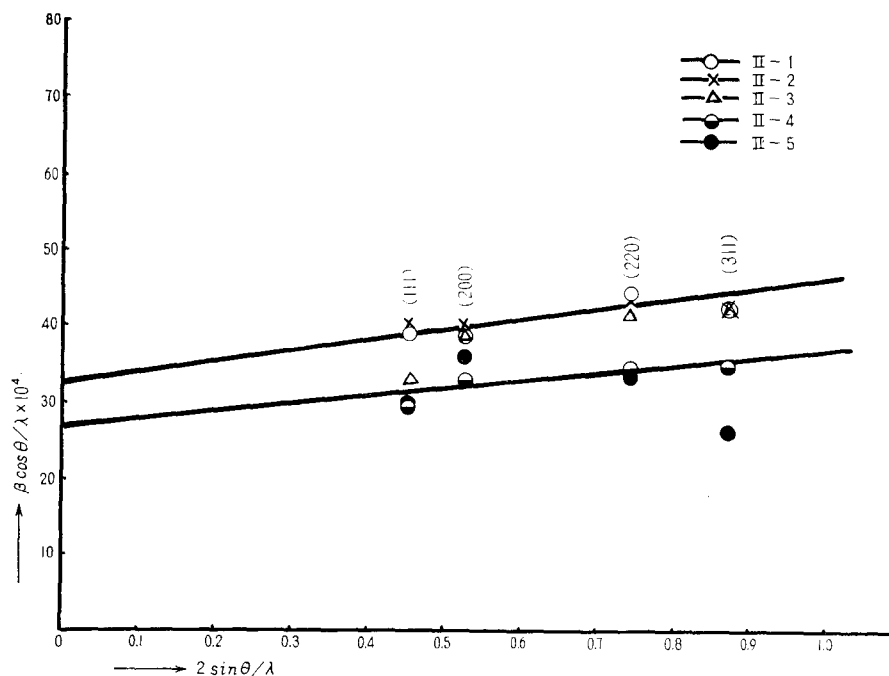


Fig. 4 (a). Variation of  $\beta \cos \theta / \lambda$  with  $2 \sin \theta / \lambda$  for  $r'$ -phase of Catalyst-II.

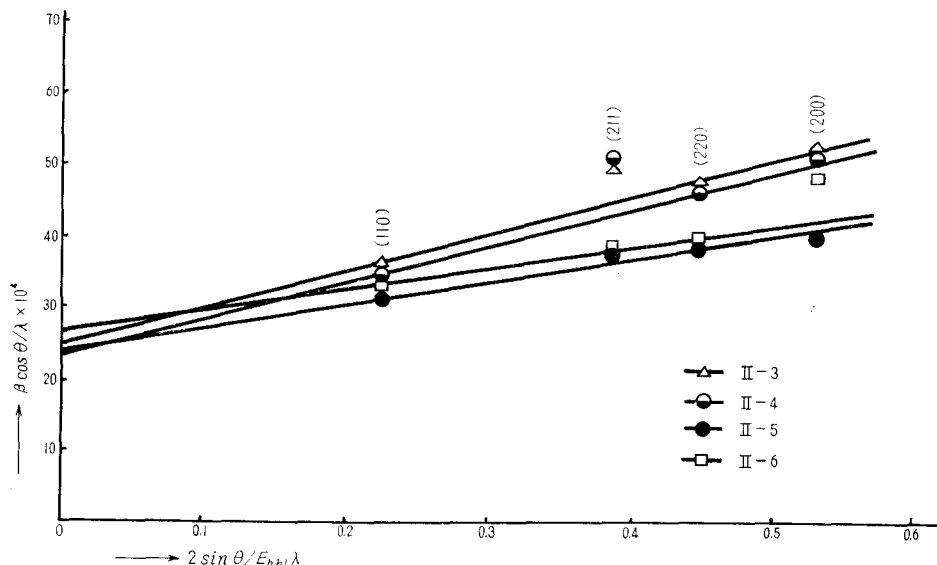


Fig. (4) b. Variation of  $\beta \cos \theta / \lambda$  with  $2 \sin \theta / E_{hkl} \lambda$  for  $\alpha$ -phase of Catalyst-II.

As seen in the Table, both the phases of  $\gamma'$  and  $\alpha$  in Catalyst-I, -II and-III appear to show no changes in crystallite size beyond the limits of experimental error along the line of flow, the crystallite size being estimated from the intercept of straight lines in Figs. 3, 4 and 5 at about 3300 Å for Catalyst-I and 400 Å for Catalyst-II and-III. The observed lattice strain, on the other hand, was somewhat complicate;  $\eta$  of  $\gamma'$ -phase in Catalyst-I is almost the same to that in Catalyst-II and remains almost constant both in the cases along the line of flow, whereas that of  $\alpha$ -phase in Catalyst-II decreases, as seen in the Table, towards the outlet of the bed but that in Catalyst-III remains almost constant along the flow. The decrease of lattice strain observed with  $\alpha$ -phase in Catalyst-II may be attributable to the decrease in fraction of coexistent  $\gamma'$ -phase which gives rise to lattice strain in the  $\alpha$ -phase by misfit of  $(112)_{\gamma'}$  or  $(110)_{\gamma'}$ , respectively with  $(210)_{\alpha}$  or  $(001)_{\alpha}$ , which is respectively parallel to the former<sup>10</sup>.

In case where the catalyst is composed solely of  $\gamma'$ -phase or  $\alpha$ -phase, the observed lattice strains may result from non-uniform distribution of nitrogen in the catalyst or such distribution of promoter comprized or cold work or from some or all of them. The observed intensity decrease was explained in 1., § 3 on the basis of "frozen heat motion", assuming uniform distribution of the excess nitrogen atoms in  $\gamma'$ -phase in Catalyst-I. Admitting the latter uniform distribution in  $\gamma'$ -phase in Catalyst-I as well as in Catalyst-II, the lattice strain observed in these cases may be attributed to either or both of the

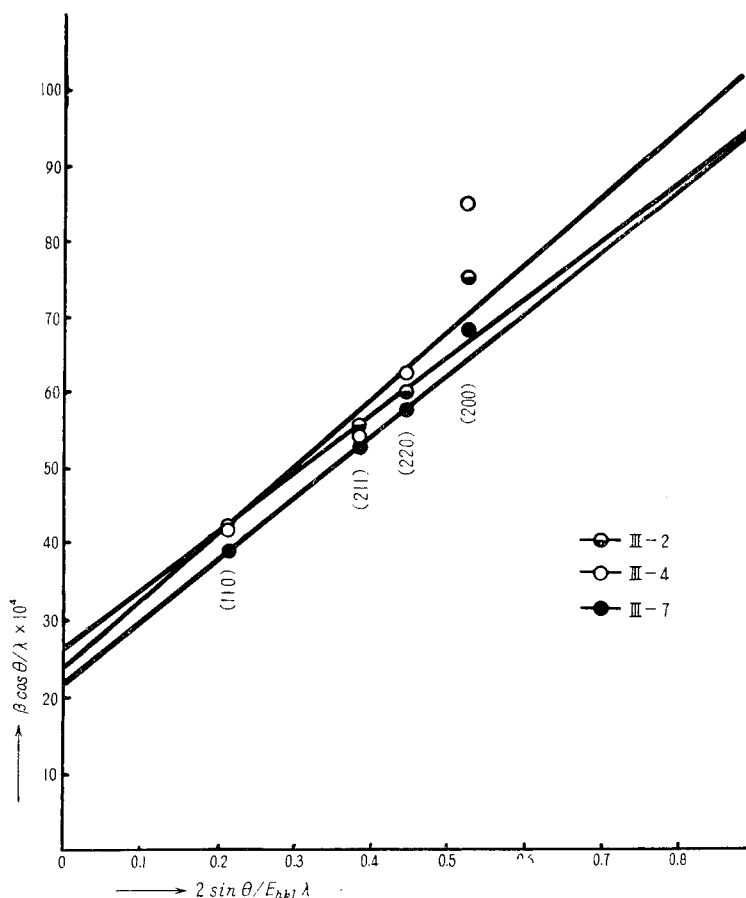


Fig. 5. Variation of  $\beta \cos \theta / \lambda$  with  $2 \sin \theta / E_{hkl} \lambda$  for  $\alpha$ -phase of Catalyst-III.

non-uniform distribution of comprized promoters and the cold work. If then, the effect of promoter should be predominant in case of  $\gamma'$ -phase in Catalyst-I, since the lattice strain of the latter without cold work is almost the same as that of the  $\gamma'$ -phase in Catalyst-II with cold work. In case of  $\alpha$ -phase on the other hand the lattice strain must have resulted at least partly from the cold work, inasmuch as it is less in coarsely powdered catalyst than in finely powdered one as shown in the last line of the Table.

Figs. 4 (b) and 5 show that either the (211)- or (200)-reflection from  $\alpha$ -phase is anomalously broader than the other reflections according as  $\gamma'$ -phase coexists or not. Such anomaly of (200)-reflection was also reported by a number of workers for low carbon steel<sup>11)</sup> and filed iron<sup>12)</sup> and that of (211)-reflection for hydrogen charged iron<sup>13)</sup>. These anomalies could be elucidated by more detailed

investigation of line-profile with  $\alpha$ -iron bearing nitrogen or hydrogen.

### Summary

1. The catalysts were examined by x-ray diffraction at three typical points on the hysteresis loop of the rate of steady decomposition of ammonia, revealed by decreasing and then increasing constant hydrogen inflow rate  $N_H$  stepwise at fixed inflow rate of ammonia  $N_A$  over doubly promoted iron catalyst kept at constant temperature around 450°C. The catalysts examined were the same as those in the previous work, *i.e.* that (Catalyst-I) at point  $N_H/N_A=0$ , that (Catalyst-II) at point  $N_H/N_A=1$  on the lower curve of the loop observed on increasing  $N_H$  and that (Catalyst-III) at point  $N_H/N_A=1$  on the upper one of the loop observed on decreasing  $N_H$ .

2. The integrated intensity of each reflection from the constituent phases of consecutive layers of catalyst across the line of flow of reactant gas was observed. The observed increase of integrated intensity along the line of flow in case of the  $\gamma'$ -phase of Catalyst-I was found to be attributable to decrease of excess nitrogen over the stoichiometric composition of  $\text{Fe}_3\text{N}$ , which gives rise to the "frozen heat motion". The root mean square displacement of iron atom of the  $\gamma'$ -phase coexistent with  $\epsilon$ -phase was estimated at 0.13 Å to 0.14 Å. The gradual decrease of integrated intensity towards the outlet of the bed observed with the  $\alpha$ -phase in Catalyst-III was not similarly explicable as in the case of  $\gamma'$ -phase in Catalyst-I or -II.

3. The observed line-broadening was analyzed by CAUCHY's relation and shown to be attributable to small size of crystallite as well as to lattice strain both in the cases of  $\gamma'$ - and  $\alpha$ -phases. The lattice strain observed with the present catalyst was concluded to be due mainly to the promoter comprized in the catalyst or the cold work of powdering the catalyst for preparation of x-ray specimen respectively in the case of  $\gamma'$ -phase or  $\alpha$ -phase.

### Acknowledgments

The authors wish to thank Professor J. HORIUTI, the director of this Institute, for encouragement and helpful discussions throughout the course of this work and Dr. S. HARIYA for the use of "Norelco".

### References

- 1) I. TOYOSHIMA and J. HORIUTI, This Journal, **6**, 146 (1958).
- 2) T. MATSUI and I. TOYOSHIMA, *ibid.*, **10**, 105 (1962).
- 3) S. ENOMOTO and J. HORIUTI, This Journal, **2**, 87 (1952).

- J. HORIUTI and I. TOYOSHIMA, *ibid.*, **5**, 120 (1957).  
J. HORIUTI and I. TOYOSHIMA, *ibid.*, **6**, 68 (1958).
- 4) K. H. JACK, Proc. Royal Soc., **A 195**, 34 (1948).
  - 5) H. HENGSTENBERG and H. MARK, Naturwissenschaften **17**, 443 (1929); Z. Phys., **61**, 435 (1930); Z. Electrochem., **37**, 524 (1931).
  - 6) F. W. JONES, Proc. Royal Soc., **A 166**, 16 (1938).
  - 7) A. R. STOKES and A. J. C. WILSON, Proc. Phys. Soc. (London), **56**, 174 (1944).
  - 8) W. H. HALL, Proc. Phys. Soc., **A 62**, 741 (1949).
  - 9) W. H. HALL and C. K. WILLIAMSON, Proc. Phys. Soc. (London), **B 64**, 937 (1951).
  - 10) R. F. MEHL, C. S. BARRETT and H. S. JERABEK, Transaction AIME., **113**, 211 (1934).  
G. R. BOOKER, *et al.*, J. Iron and Steel Inst., **187**, 205 (1957).
  - 11) R. A. SMITH, *ibid.*, **163**, 147 (1953).
  - 12) R. E. SMALLMAN, Ph. D. Dissertation, Univ. Birmingham, England, (1953).
  - 13) J. PLUSQUELLEC, P. AZOU and P. BASTION, Compt. rend., **244**, 1195 (1957).  
A. S. TELELMANN, C. N. J. WAGNER and W. H. ROBERTSON, Acta Metallurgica, **9**, 205 (1961).